BHR Group
EXPERTS IN FLUID ENGINEERING

Heat Transfer of Couette Flow in Micro-channels: an Analytical Model of Seals

Sarah Shabbir [a, b], Seamus D. Garvey [b], Sam M. Dakka [b] Benjamin C. Rothwell [b]

[a]*Institute of Aerospace Technology, University of Nottingham, Nottingham, United Kingdom*
[b]*Gas Turbine and Transmission Research Centre, Department of Mechanical, Materials and Manufacturing Engineering, University of Nottingham, Nottingham, United Kingdom*

ABSTRACT
Analytical solutions of the temperature profile of a fluid in a Couette flow between two parallel plates are reported. The upper plate moves in the direction of the flow with a constant velocity and the lower plate is stationary, to simulate the conditions of a stationary seal mounted on a rotating shaft. The energy equation is solved for steady-state, laminar flow, taking into account the viscous dissipation effect of the flow due to the high shear rate of the fluid and rotational speeds being studied. An imposed temperature gradient between the two plates is used as well. The solutions use different boundary conditions of no-slip condition and a first-order slip to study the effect on the temperature profile as a result of the first-order slip condition. Brinkman number and temperature difference between the plates is also varied to see how it influences the temperature profile in the gap between the seal and the shaft. These parameters and boundary conditions influence this temperature profile. Results illustrate how slip boundary conditions at the wall show a control of the temperature rise in the annuli, resulting in reduced energy accumulation within the annuli.

NOMENCLATURE

I	Length scale of molecular structure
E	Length scale of surface roughness
L	Length scale of bulk fluid
k_s	Sand-grain roughness
dH	Hydraulic Diameter
Br	Brinkman Number
AFM	Atomic Force Microscopy
Kn	Knudsen Number
DSMC	Direct Simulation Monte Carlo
D_{CF}	Constricted Flow Diameter
D_t	Base Diameter
ϵ	Roughness
y	Normal direction distance
z	Axial Distance
u	Velocity
P	Pressure
b	Distance between the two plates

μ	Dynamic Viscosity
k	Thermal Conductivity
q	Heat flux
h	Co-efficient of heat transfer
T	Temperature
T_o	Initial Temperature
T_b	Temperature in the annuli
V	Velocity of the top plate
τ	Tangential momentum (initial, reflected, wall)
λ	Mean Free Path
$\bar{u}$	Dimensionless velocity
$\bar{y}$	Dimensionless distance
S	Source term
ρ	Density
σ_v	Tangential momentum accommodation co-efficient
R_a	Roughness average
R_p	Maximum profile peak height
R_{sm}	Mean spacing of profile irregularities
F_p	Floor distance to mean line
c_p	Specific heat capacity
η	Normal direction to the wall
u_s	Slip velocity
l_s	Slip length

1 INTRODUCTION

In recent years, fluid flow through micro-channels has been given great significance, as heat transfer through such channels is dependent on physical properties of the flow like geometry and boundary conditions, among others. In fact, it is mainly these channels' surface roughness that helps not only achieve an effective seal [1, 2], but also impacts heat and viscous heat dissipation within the channel. An example of this is the fluid flow of an annulus between two cylinders, a common occurrence in engineering. When the innermost of these cylinders is rotating and the other is stationary, heat is generated within the annulus due to the viscous motion of the fluid layers slipping past each other. The rotation of the inner cylinder results in a high velocity gradient of the annulus fluid, manifesting as a significant temperature rise. Here, this model represents a stationary seal mounted on a rotating shaft with an interference fit to study the flow of a 1-10 micron thin layer of lubricant within the annulus. Specific parameters of turbine engine oil, Aeroshell 555 are considered in this analysis.

The sealing mechanisms of radial lip seals is investigated from a thermal analysis perspective, to study the presence of viscous heat generation and its potential role in how seals work. This model studies the rise in temperature effect of viscous dissipation in the annulus, demonstrating how changing certain conditions can alter the temperature profile across the annuli.

Previous studies employing experimental and numerical analysis of viscous dissipation in micro-flows drew the following conclusions on its impact on the flow [3-5]:

i. The viscous dissipation effect becomes more prominent, especially on the friction factor as the dimension of the system being studied decreases below 50

microns. Neglecting to account for it in micro-conduits can result in skewed results.

ii. As channel size decreases, viscous dissipation effects will increase and they should be considered in cases with imposed boundary heat sources as well.

iii. Some key factors that play a critical role in determining the extent of impact of the viscous dissipation on the flow are the Reynolds number, Brinkman number and channel dimensions. Fluids that are highly viscous and have a low specific heat capacity will still experience strong viscous dissipation effects, even if they are laminar with a low Reynolds number.

iv. Aspect ratio of the channel and overall geometrical parameters also contribute to the effect of viscous dissipation. In particular, channels with an aspect ratio that moves away from unity will experience an increased effect. .

In regards to solid-wall proximal motion, three relevant length scales exist [1]: i) I, length scale associated with the molecular structure of the fluid (this is irrelevant as it is dimensionally not comparable), ii) E, length scale associated with the solid surface roughness, and iii) L, length scale associated with the fluid's bulk motion. It can be the dimension of the channel or diameter of the tube through which the fluid flows. In this case, L is comparable in size to E. Hence, the difference in flow between that in micro-channels and macroscopic scales is due to a) the predominance of molecular effects in a small scale, and b) the extreme amplification of the magnitudes of ordinary continuum parameters. It has been previously mentioned [7] that thermal effects may play an important role in sealing performance. However, such investigations are not always included in the current analysis of seals.

2 FLOW BETWEEN TWO PARALLEL PLATES – NO SLIP BOUNDARY CONDITION

The annuli is very small in comparison to the radius and the radial system has been modelled as a planar system for simplification. We are studying micro channels and as the dimension of the channels being analysed are scaled down, the viscous dissipation effect is of critical importance. This is known as the scaling effect in a micro-flows and becomes prominent in flows where L is less than 100 microns. Fluid flow through such micro-channels and microfluidic devices is characterized by a very high velocity gradient due to the channel dimension. Hence, viscous effects will be high, irrespective of the Prandtl number the flow [2]. This study is carried out to analyse the heat transfer mechanism in the system and the resulting temperature rise in the fluid. The thermal response of the fluid for different brinkman numbers is also studied.

A Couette flow is shown below where one plate is moving with a velocity V m/s and the other plate is stationary. This will result in a linear velocity profile as shown below. If a negative pressure gradient is also imposed, then the velocity profile will be parabolic in nature. The type of flow being studied here is a simple Couette flow.

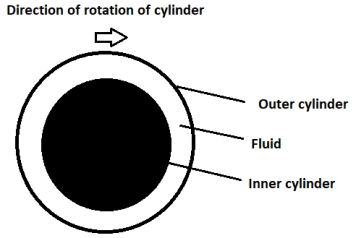

Figure 1a: Flow between two rotating cylinders

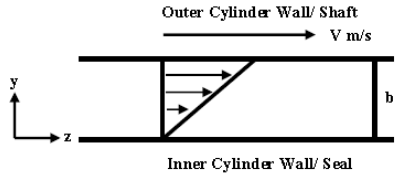

Figure 1b: Flow between two parallel plates

2.1 Velocity Profile

To model the velocity profile, a combined Couette-Poiseuille flow is considered to derive the full velocity equation and the parabolic term with pressure gradient can be equated to zero to get the linear Couette flow profile. For the combined flow, the Navier stokes equations are used with the boundary conditions changed for one moving plate.

$$\mu \frac{d^2u}{dy^2} = \frac{dP}{dz}$$

$$\int \frac{d^2u}{dy^2} dy = \frac{1}{\mu} \int \frac{dP}{dz} dy$$

$$u = \frac{1}{\mu}\left(\frac{dP}{dz}\right)\left(\frac{y^2}{2}\right) + c_1 y + c_2$$

Boundary conditions

1) $at\ y = 0, \quad u = 0$
2) $at\ y = b, \quad u = V\frac{m}{s}$

For 1) $c_2 = 0$
For 2) $c_1 = \frac{V}{b} - \frac{b}{2\mu}\left(\frac{dP}{dz}\right)$

$$u = \frac{1}{2\mu}\left(\frac{dP}{dz}\right)(y^2 - by) + \frac{Vy}{b} \quad \textbf{Equation (1)}$$

Equation 1 is the final equation that describes the velocity profile within the annuli. The first term is the parabolic term describing the Poiseuille element of the flow and the second term is the linear term describing the Couette flow. Flow the Couette only flow, the first term can be set to 0 as the pressure gradient $\frac{dP}{dz} = 0$. Note that this is pressure in the circumferential direction and is not relevant to the application of sealing.

To model the velocity profile, dimensionless parameters can be introduced where equation 2 is the non-dimension equation for velocity that is plotted in figure 2.

$$\bar{u} = \frac{u}{V}, P = -\frac{b^2}{2\mu V}\left(\frac{dP}{dz}\right), \bar{y} = \frac{y}{b}$$

$$\frac{u}{V} = \left(\frac{y}{b}\right)\left[1 - \left(\frac{b^2}{2\mu V}\right)\left(\frac{dP}{dz}\right)\left(1 - \frac{y}{b}\right)\right]$$ **Equation (2)**

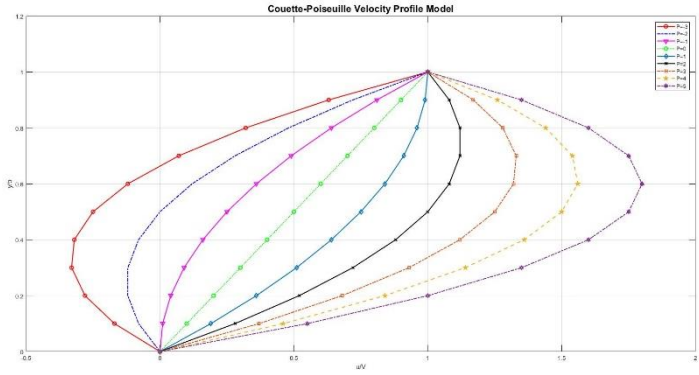

Figure 2: Velocity Profile Couette & Couette-Poiseuille Flow

$P = 0$ is the case of simple Couette flow, which is the only case relevant to the application of sealing. Figure 2 displays the velocity profile for positive and negative pressure gradient in the system by changing the values of dimensionless pressure gradient P. This analysis has been done in an attempt to verify the analytical solution and equations being derived with previous analysis done by [3] on a Couette-Poiseuille case. Turbine engine oil is taken as the fluid being analysed in the annuli and its properties are considered (Aeroshell 555). The dimensions are considered of an annuli of 1-10 microns with a shaft and seal radius of ~ 49-50 mm.

2.2 Heat Transfer

Considering the thermal analysis of the system, as the outer cylinder rotates, heat is generated within the fluid due to the viscous dissipation. This dissipation is a result of the adjacent layers of the fluid slipping past one another with a very high velocity gradient and turns mechanical and kinetic energy into heat energy. It is then accounted for as a significant rise in the temperature of the fluid as thermal energy is generated in the fluid [4]. As can be seen in equation 3, it will appear in the energy equation as the source term in the fluid flow. The importance of viscous dissipation in a flow can be quantified by a dimensionless number known as the Brinkman number. It is used to account for the unusual heat transfer behaviour in micro channels, particularly because they drastically differ from the behaviour of conventionally sized channels.

The heat generation term is a function of the velocity profile. The source term, $S = -\tau_{zx}\left(\frac{\partial u}{\partial y}\right)$ where $\tau_{zy} = -\mu\left(\frac{\partial u}{\partial y}\right)$. Hence, the viscous term in the energy equation is given as $S = \mu\left(\frac{\partial u}{\partial y}\right)^2$. To derive the viscous term in the energy equation, we first need the velocity equation as seen in the formulae above.

The final energy equation is equation 3 below:

$$\frac{\rho c_p \Delta T}{\Delta t} = k\nabla^2 T - T\left(\frac{\partial P}{\partial T}\right)\nabla V + S$$ **Equation 3**

In this case, we will neglect the convection term and assume that the main mode of heat transfer is conduction as the flow is laminar and not turbulent. The expansion effects are also neglected and we assume that density is not a function of temperature. The density and viscosity of the engine oil can be assumed to vary with pressure, however the pressures experienced in this case are almost insignificant and can be assumed to be low enough to be unable to alter the properties of the bulk flow. Only Couette flow is considered here to get the temperature rise through the annuli

Where $u = \frac{V}{b}y \; and \; \frac{du}{dy} = \frac{V}{b}$

$$\frac{dq_y}{dx} = \mu\left(\frac{V}{b}\right)^2$$

$$q = -\frac{k\partial T}{\partial y} = h\Delta T$$

Boundary conditions:
1) $at\ y = 0, \quad T = T_o$
2) $at\ y = b, \quad T = T_b$

$$\frac{d}{dy}\left(-\frac{k\partial T}{\partial y}\right) = \mu\left(\frac{V}{b}\right)^2$$

$$-\frac{k\partial T}{\partial y} = \mu\left(\frac{V}{b}\right)^2 y + c_1$$

$$\int \frac{\partial T}{\partial y} = -\int \frac{\mu}{k}\left(\frac{V}{b}\right)^2 (y) + \frac{c_1}{k}$$

$$T = -\frac{\mu}{k}\left(\frac{V}{b}\right)^2\left(\frac{y^2}{2}\right) - \frac{c_1}{k}y + c_2$$

Applying the BC's

1) $c_2 = T_o$
2) $T_b = -\frac{\mu}{k}\left(\frac{V}{b}\right)^2\left(\frac{b^2}{2}\right) - \frac{c_1}{k}b + T_o$

$$c_1 = -\frac{k}{b}(T_b - T_o) - \frac{\mu}{b}\left(\frac{V^2}{2}\right)$$

$$T = -\frac{\mu}{k}\left(\frac{V}{b}\right)^2\left(\frac{y^2}{2}\right) + \frac{k}{b}(T_b - T_o)\left(\frac{xy}{k}\right) + \frac{\mu}{b}\left(\frac{V^2}{2}\right)\left(\frac{y}{k}\right) + T_o$$

Where dimensionless Brinkman number $Br = \frac{\mu V^2}{k(T_b - T_o)}$

$$\frac{T - T_o}{T_b - T_o} = \frac{y}{b} + \frac{1}{2}Br\frac{y}{b}\left[1 - \frac{y}{b}\right] \quad \textbf{Equation (4)}$$

Equation 4 dictates the temperature rise through the annuli for simple Couette flow case and $\Delta T = T_b - T_o$. The Brinkman number is an indication of the importance of the viscous heat generation with respect to the heat that will flow due to an imposed temperature difference. As the Brinkman number increases, the effect of viscous dissipation becomes more apparent. When Br > 2, the point of maximum temperature will move toward the centre of the annulus, resulting in a more parabolic temperature profile rather than linear

due to the temperature rise. The equation derived governing temperature distribution is solved for different Br & ΔT with oil as the fluid in the annuli

Figures 3, 4 and 5 below show the temperature variations across the width of the annuli with the dimensionless distance $\frac{y}{b}$ for a brinkman number of 0.2, 2 and 4. The ΔT is varied to observe the temperature in the annuli because of differences in wall temperatures. As seen in figure 3, for a Br = 0.2, the temperature in the annuli increases as the dimensionless distance increases toward the centre of the annuli. Note that the rate of temperature rise is seen to increase with increasing ΔT. This indicates that the heat conduction due to the imposed temperature gradient across the annulus is dominating the temperature profile over the viscous generation, and therefore the mechanism of heat transfer in the system. In figure 3, the temperature profiles for Br = 2 are similar to those corresponding to Br = 0.2. However, in this case, the temperature profile in the annuli becomes parabolic rather than linear. This indicates that the heat energy generated due to viscous dissipation in the annuli results in a rise of the fluid temperature. Therefore, the temperature gradient decreases as y/b increases and approaches the moving wall which is the outer rotating cylinder. The temperature in the fluid here approaches that of the rotating wall, reducing the heat transferred from the rotating cylinder to the fluid. As an equilibrium temperature is reached between the fluid and the rotating cylinder, there is little to no heat conduction observed. As seen in figure 5, for the final case of Br = 4, the temperature profile becomes even more parabolic at the ΔT increases and it reaches its maximum at y/b $\sim$ 0.75. This can be attributed to a higher rate of viscous heat dissipation in the fluid and therefore, the fluid temperature increases more than the temperature of the wall. For this final case, the amount of heat generated results in the fluid reaching a higher temperature than that of the rotating cylinder, which can be seen below.

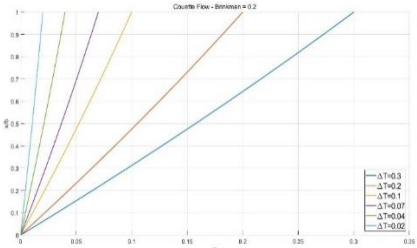

Figure 3: Br=0.2 (Couette Flow Case 1)

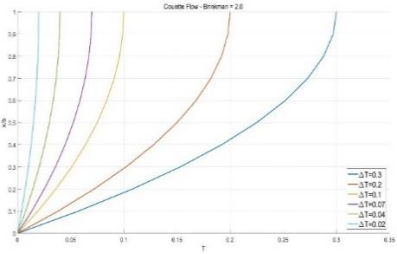

Figure 4: Br= 2 (Couette Flow Case 1)

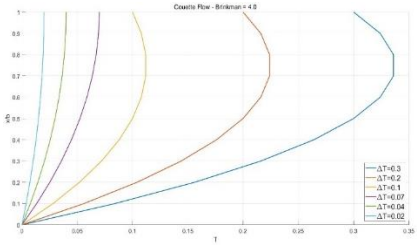

Figure 5: Br = 4 (Couette Flow Case 1)

3 FLOW BETWEEN TWO PARALLEL PLATES–SLIP BOUNDARY CONDITION

A similar flow is modelled to the previous case, but with different boundary conditions to include the surface roughness and slip boundary conditions to investigate the effect it will have on the temperature profile across the annulus. As mentioned in the introduction, since the L is comparable in size to E, this means that the surface roughness effects will be prominent enough that they must be considered – even in laminar flow. While traditional theory neglects roughness effects in laminar flow, recent literature suggests that in micro-flows, the effects of surface roughness should be included [5][6]. Since the annuli being considered is a few microns thick, calculation of the Knudsen number suggests that it may not lie within the classical continuum flow regime and slip must be applied at the boundary conditions [7]. Intuitively, we would expect that the surface roughness would reduce the effect of slip flow – however, since the cohesive forces between the liquid are able to overcome the adhesive forces between the liquid and solid wall, they can manage to detach from the surface and exhibit slip at the wall. The shear effect within this fluid is also very high, which is why the viscous term can be considered to begin with. This will also help the bulk liquid detach from the wall and pull the liquid particles along with them, possibly resulting in finite slip at the stationary wall.

3.1 Velocity Profile

To include roughness effects and to incorporate the Knudsen number regime of the flow in this analytical model [8]

(i) the flow area constriction theory is used and
(ii) Increase in the wall shear stress by using a velocity slip boundary condition.

To successfully implement (i), AFM (atomic force microscopy) and a ZETA profilometer was utilized to test for the roughness profile of samples of specimens to obtain the values that are relevant to this application. Surface roughness parameters were found for the specimens to ensure that they fall within the desired range of suggested roughness for aerospace seals. The data from those tests are used here. The constricted flow theory proposed by [8] is summarized and applied as follows. Different roughness heights would mean that the flow separation of the fluid would be different and in each case, the flow would or would not re-attach to the wall. The new flow boundary established as a result of this roughness element exceeding a certain size is now suspended above the actual pipe wall at a distance supposedly named y away from the pipe wall. The effectively diameter of the flow is then reduced by the presence of the surface roughness elements on the surface of the tube and this lays the foundation of Kandlikar's constricted flow theory. The exact value of y is not known, but can be found through data in the following manner. It is bounded between 0 and the height of the roughness and sits somewhere in between these two values. The new effective flow diameter can then be based on the constricted flow, $D_{CF} = D_t - 2\epsilon$

This is assuming the new value suggested as y closely resembles ϵ, the value suggested by Nikuradse [9] in his sand grain experiments to quantify surface roughness and is the pioneer of the relative roughness values established in the moody chart. Here, D_{CF} is known as the constricted flow diameter, D_t is known as the base diameter of the actual pipe and ϵ is known as the average roughness height. An approach that is used in rarefied gas flow dynamics is to introduce a slip velocity boundary condition after roughness effects and parameters are included and a similar approach is taken in this case.

To successfully account for the wall shear stress in (ii), a slip velocity boundary condition is then introduced once the roughness features have been defined as mentioned above.

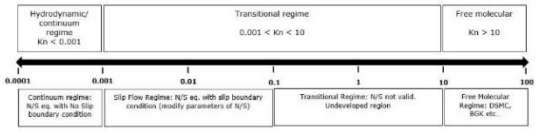

Figure 6: Knudsen number regimes

The Knudsen number represents how rarefied the fluid flow system is where $Kn = \frac{\lambda}{L}$
$\lambda = mean\ free\ path, L = charactertistic\ length\ of\ bulk\ flow\ motion$

For Knudsen numbers < 0.001, the system is considered to be in a continuum state as seen in figure 9 above. This means that Navier-Stokes equations can be applied with a no-slip boundary condition. However, as the system becomes more rarefied, it moves further along on the spectrum. In the first part of the transitional regime where 0.001 < Kn < 0.1, the Navier-stokes equations are still valid – however a slip velocity must be applied as a no-slip condition is ideal and unrealistic. A first order slip velocity is known to be sufficient for this regime and for the second half of the transitional regime, higher order slip conditions may be valid amongst other models. Maxwell's slip equation can be expanded to second and third order, however we use a first order model here. $u_g = u_w + \alpha Kn + \beta Kn^2 + \cdots$
For the case of the shaft and seal, we assume the mean free path of air $\lambda_{AIR} = 68\ nm, L = 1 - 10\mu m\ \ \&\ \ Kn \sim 0.022$ for this system as an approximation since it is not possible to know the mean free path of the actual system. We can only assume that due to the scale of L, we may be in a slightly rarefied state. Further, surface roughness effects have been shown to introduce a finite slip at the boundary [10].

The rarefaction of a system does not only depend on the mean free path of the system it also depends on the length scale. Extremely small channels i.e. micro channels can compensate for a not so low mean free paths and result in a higher Knudsen numbers which can be the case here. When Knudsen numbers are on the higher side (or in the transition regime), the Knudsen layer becomes significant. It is the sublayer at the surface interface a few mean free path thick. In such cases, collision frequency is low because the channel is so small and therefore equilibrium between the velocity and temperature near the wall cannot be easily established whilst considering the macro flow. We use no-slip boundary conditions to see how it will affect the temperature profile in the annuli.

The simplest extension to the no-slip boundary condition is the simplistic Navier slip where the boundary velocity is proportional to the velocity gradient. Maxwell's first order slip boundary condition and Navier's slip theory aligned well as they were the same concept, presented differently. Maxwell's equation for first order slip flow is

$u_g - u_w = \frac{2-\sigma_v}{\sigma_v}\left[\lambda \frac{\partial u}{\partial y}\right]$, $where\ \sigma_v = \frac{\tau_i - \tau_r}{\tau_i - \tau_w}$
$u_s = u_g - u_w$

The slip velocity in terms of a physical system can be defined as the tangential velocity one mean free path away from the wall [7]. σ_v is the tangential momentum accommodation coefficient. It can be said that the slip velocity can be defined as the mean velocity of the layer of fluid one mean free path away from the wall. Therefore, a higher proportion of specular reflections will result in higher slip velocity as well. This definition is relevant to slightly rarefied systems as a longer mean free path will result in the presence of fluid-solid collisions near the surface [11]. The effect of varying the tangential momentum accommodation co-efficient on the velocity in this system is presented here. The final

equations for the slip flow boundary conditions in non-dimensional form are presented below.

For Couette flow with first order slip, the solution is:

$$u^* = \frac{1}{1+2\alpha} y^* + \frac{\alpha}{1+2\alpha}$$

Where $\alpha = \frac{2-\sigma_v}{\sigma_v} Kn$

$$u^* = \frac{u}{V}, y^* = \frac{y}{b}, Kn = \frac{\lambda}{L}$$

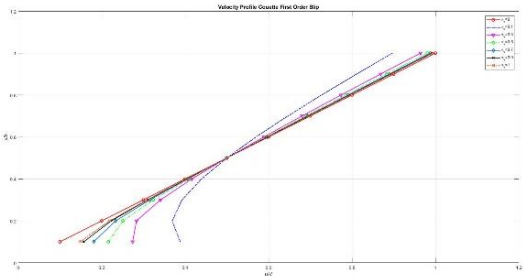

Figure 7: Velocity profile for Couette first order slip

As seen in figure 10 above, a slip velocity results in a steeper gradient on the velocity graph with a 'slip' at the boundary. The tangential momentum accommodation co-efficient is seen to vary and the degree of slip based on the value of σ_v can be seen. The $\sigma_v = 0.1$ presents with the highest slip as explained above that a higher proportion of specular reflections results in higher slip velocity.

Following this, the non-dimensional equation of the micro-Couette flow with first order slip is equation 6 below.

$$u = \frac{v}{b} \cdot \frac{1}{1+2\alpha} y + \frac{v\alpha}{1+2\alpha}$$ **Equation 5**

3.2 Heat Transfer

Once the equation for micro Couette flow with velocity slip boundary equations has been derived, this section aims to study the effect of incorporating the Knudsen number and surface roughness in the analytical model to see the effect on temperature variation in the fluid as a result of viscous dissipation effect and constricted flow theory.

$$u = \frac{v}{b} \cdot \frac{1}{1+2\alpha} y + \frac{v\alpha}{1+2\alpha}$$

$$\frac{du}{dy} = \frac{V}{b(1+2\alpha)}$$

The energy equation with the viscous dissipation term is presented below.

$$\frac{dq_x}{dx} = \mu\left(\frac{V}{b(1+2\alpha)}\right)^2$$

Boundary conditions:
1) $at\ y = 0, \quad T = T_o$
2) $at\ y = b, \quad T = T_b$

$$\frac{d}{dy}\left(-\frac{k\partial T}{\partial y}\right) = \mu\left(\frac{V}{b(1+2\alpha)}\right)^2$$

$$\frac{T-T_0}{T_b-T_o} = \frac{y}{b} + \frac{1}{2}Br\left(\frac{y}{b}\right)\left(\frac{1}{(1+2\alpha)^2}\right)\left(1-\frac{y}{b}\right)$$

$$\frac{T-T_0}{T_b-T_o} = \frac{y}{b} + \frac{1}{2}Br\left(\frac{y}{b}\right)\beta\left(1-\frac{y}{b}\right)$$

$$\beta = \frac{1}{(1+2\alpha)^2},\ \alpha = \frac{2+\sigma_v}{\sigma_v}Kn$$

Equation 8 dictates the temperature profile in the annuli as:

$$\frac{T-T_0}{T_b-T_o} = \frac{y}{b} + \frac{1}{2}\frac{\mu v^2}{k(T_b-T_o)}\frac{1}{\left(1+2\left(\frac{2+\sigma_v}{\sigma_v}Kn\right)\right)^2}\left(\frac{y}{b}\right)\left(1-\frac{y}{b}\right) \quad \textbf{Equation 6}$$

Following is the Couette flow with slip boundary conditions with a brinkman number of 0.2. As seen in figure 11, the effect of viscous dissipation has not taken effect here as yet and no significant temperature increase can be seen. When increasing the Brinkman number to 2 in figure 12, a slight rise in temperature is seen due to the viscous generation within the annuli. However, due to the presence of the slip term, the temperature rise is controlled. If it is compared to the Couette flow case without the slip (as it will be in the discussion), the curve is more parabolic in nature due to the heat generation. The same effect is not seen here even though the exact same dimensions and conditions are kept with the exception of the slip term being included. Further increasing the Brinkman number to a value of 4 as seen in figure 13 results in a slightly more parabolic curve. However, the temperature rise is again controlled to a large extent as seen in the graph below. The true parabolic nature of the Couette flow is not observed as it is earlier.

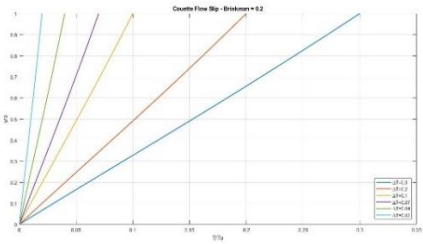

Figure 8: Br = 0.2 (Couette Flow Case 2)

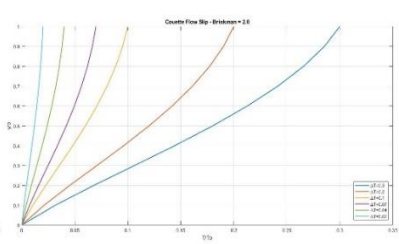

Figure 9: Br = 2 (Couette Flow Case 2)

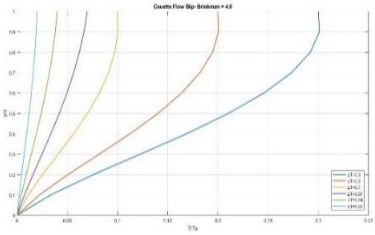

Figure 10: Br = 4 (Couette Flow Case 2)

4 DISCUSSION

4.1 Couette-flow – Slip vs no Slip BC's

Incorporating a slip velocity boundary condition to model the problem in the right Knudsen number regime along with accounting for roughness on the surface results in a clear control of the rise in temperature within the annuli. The viscous dissipation effect is controlled to a certain extent as seen when you compare between figure 14 and 15. All conditions are kept constant – however in the second model we have modified the Navier Stokes equations by adding a first order slip boundary condition. We note that the temperature rise due to viscous heat dissipation is not as profound.

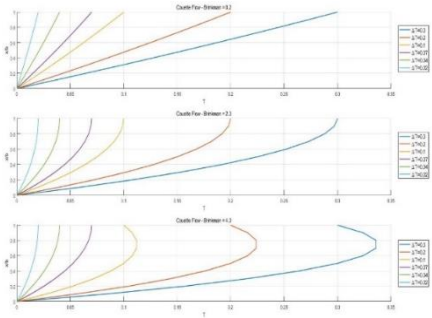

Figure 11: No-Slip BC – Couette flow heat transfer

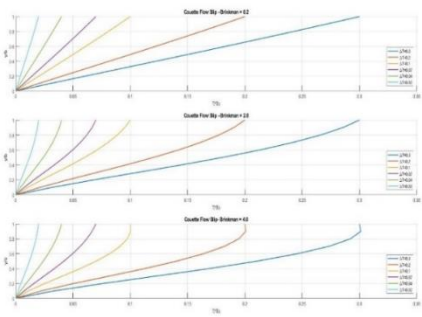

Figure 12: Slip BC – Couette flow heat transfer

As can be seen in figure 14 and 15 above, there is clear control over the temperature rise and viscous dissipation effect with the addition of the slip at the boundary conditions. Even with a brinkman number of 4, it is evident when compared to the profile in figure 14, that the heat generation in the annuli of figure 15 is limited. This suggests that the slippage is limiting the temperature rise by some means. Looking at the final equation,

$$\frac{T-T_0}{T_b-T_o}=\frac{y}{b}+\frac{1}{2}Br.S.\left(\frac{y}{b}\right)\left(1-\frac{y}{b}\right)$$

Where $Br=\frac{\mu v^2}{k(T_b-T_o)}$, $S=\frac{1}{\left(1+2\left(\frac{2+\sigma_v}{\sigma_v}Kn\right)\right)^2}$

In this case, Br and S are the two terms that can dominate the thermal behaviour of the fluid across the annulus. One circumstance of the flow is where the brinkman number dictates the flow, dominated by temperature rise due to viscous effects. The other

circumstance is when the slip effect is introduced through the tangential momentum accommodation coefficient and the roughness effect dictates the thermal behaviour of the fluid. Following this, a possible explanation is hypothesized in the following section.

4.2 Effect of Surface Roughness

The association of surface roughness with slip is still under debate as there is contradicting research regarding it. While some research associates slip with smooth surfaces, assuming that a smoother wall will enhance slip, other work suggests quite the opposite. In many cases, a surface roughness is seen to enhance the effect of slip and results in a higher slip velocity [10], especially in flows that are not in a fully continuum regime and are slightly rarefied.

As a result of including the tangential momentum accommodation coefficient, Knudsen number and slip conditions, a clear control over the viscous dissipation effect is observed. The effect is seen subdue to heat generation by offsetting the effect of the rising brinkman number as the shear in the fluid increases. The viscous dissipation effect is found through the gradient of the velocity profile, as seen in section 3.2. Therefore, introducing a slip velocity would change the gradient of this velocity profile as it is no longer meeting the zero velocity condition at the boundary. Surface roughness is presumed to play a critical role for this control in energy accumulation at the surface, contributing to the finite slip at the boundary. The temperature control would indicate that the local viscosity of oil would not decrease as it would if the temperature were to rise by a higher amount. This could be a deciding factor in controlling the leakage in the seal. Further, a theory regarding the presence of a thermal instability is presented.

4.3 Thermal Instability in Seals

The stability of fluid flow is a problem that has been contemplated for many decades. Fluid flows can be characterized as either stable or unstable. If a flow is stable and it is perturbed from its initial state, the flow field will return back to its original state. On the other hand, an unstable flow, when perturbed would result in a different flow field. This can also be applied to the case of a rotating shaft and a stationary seal with a film of lubricant in between these two components. Studying the fluid flow of this lubricant layer in between the shaft and seal is essential in understanding how the fluid is being sealed. For further research, this includes assessing the system from a stability standpoint to investigate whether the energy accumulation in the flow due to the viscous heat dissipation is enough to perturb the initial state of the fluid so that it will result in a different flow field.

We hypothesize that the energy feedback can result in an occurrence of a harmonic oscillation due to the instability of the flow. The maintenance of such an oscillation implies the existence of a feedback loop in the system. The presence of the instability essentially is fed by this feedback loop. The indication that a thermal instability may exist within the seal, where the state of the instability would arguably transfer between two states, each dominated by a different effect. One state would be dominated by the rising brinkman number and viscous dissipation effect. The second state would be the slip, representing the surface roughness and rarefied regime and the seal would alternate between these two states periodically, resulting in a self-oscillating instability that would not go off into infinity but would rather sustain itself, explaining some of the micro-flow mechanics behind effective sealing mechanisms. Assuming there is enough momentum in energy being accumulated in the annuli to push the system into a full 180 degree phase lag, this would explain the presence of a self-sustaining oscillation of the temperature profile within

the gap between the seal and shaft. Extended research on this is ongoing in an effort to further this hypothesis and research possibilities that may support this theory.

5 CONCLUSION

The momentum and energy equations were solved analytically for the steady state case with laminar flow of the incompressible turbine engine oil between a seal and shaft, of a Couette flow between two plates. Both cases of (a) no slip conditions and (b) first order slip condition were solved analytically and the equations dictating the temperature profile across the annuli were plotted. The results showed that the presence of viscous dissipation in micro-channels is profound with increasing Brinkman number due to the small gaps being considered and high shear flows. Viscous dissipation term cannot be neglected in the consideration of such flows and should be taken account in any thermal analysis of such seals in the future. Secondly, the effect of including slip conditions at the boundary's analytically showed a control in the temperature rise in the gap. Even with a brinkman number higher than 2, where the effect of the viscous dissipation is meant to dominate the flow, it is possible to control that effect due to the presence of a slip. Slip is associated with the micron dimensions of the annuli and it is also believed that in this case, the surface roughness is a factor that will also result in slip observed at the wall.

ACKNOWLEDGEMENTS

This work is funded by the INNOVATIVE doctoral programme. The INNOVATIVE programme is partially funded by the Marie Curie Initial Training Networks (ITN) action (project number 665468) and partially by the Institute for Aerospace Technology (IAT) at the University of Nottingham.

REFERENCES

[1] S. RICHARDSON, "On the no-slip boundary condition," *J. Fluid Mech.*, vol. 59, no. 4, pp. 707–719, 1973.

[2] S. MUKHERJEE, P. BISWAL, S. CHAKRABORTY, and S. DASGUPTA, "Effects of viscous dissipation during forced convection of power-law fluids in microchannels," *Int. Commun. Heat Mass Transf.*, vol. 89, no. November, pp. 83–90, 2017.

[3] H. MOKARIZADEH, M. ASGHARIAN, and A. RAISI, "Heat transfer in Couette-Poiseuille flow between parallel plates of the Giesekus viscoelastic fluid," *J. Nonnewton. Fluid Mech.*, vol. 196, pp. 95–101, 2013.

[4] Y. M. HUNG, "A comparative study of viscous dissipation effect on entropy generation in single-phase liquid flow in microchannels," *Int. J. Therm. Sci.*, vol. 48, no. 5, pp. 1026–1035, 2009.

[5] G. GAMRAT, M. FAVRE-MARINET, S. LE PERSON, R. BAVIÈRE, and F. AYELA, "An experimental study and modelling of roughness effects on laminar flow in microchannels," *J. Fluid Mech.*, vol. 594, no. March 2014, pp. 399–423, 2008.

[6] S. G. KANDLIKAR, "Exploring roughness effect on laminar internal flow-are we

ready for change?," *Nanoscale Microscale Thermophys. Eng.*, vol. 12, no. 1, pp. 61–82, 2008.

[7] A. BESKOK, "Validation of a new velocity-slip model for separated gas microflows," *Numer. Heat Transf. Part B Fundam.*, vol. 40, no. 6, pp. 451–471, 2001.

[8] S. G. KANDLIKAR, D. SCHMITT, A. L. CARRANO, and J. B. TAYLOR, "Characterization of surface roughness effects on pressure drop in single-phase flow in minichannels," *Phys. Fluids*, vol. 17, no. 10, pp. 1–11, 2005.

[9] N. JOHANN, "Laws of Flows in Rough Pipes," *Natl. Advis. Com. Aeronaut.*, vol. 223, no. 3, p. 403, 1950.

[10] M. SHAMS, M. H. KHADEM, and S. HOSSAINPOUR, "Direct simulation of roughness effects on rarefied and compressible flow at slip flow regime," *Int. Commun. Heat Mass Transf.*, vol. 36, no. 1, pp. 88–95, 2009.

[11] J. J. SHU, J. BIN MELVIN TEO, and W. KONG CHAN, "Fluid velocity slip and temperature jump at a solid surface," *Appl. Mech. Rev.*, vol. 69, no. 2, 2017.